one pair will then be "connected" through their ligands coordinated in the *xy* planes, i.e. the planes containing the unpaired electrons. Figure 3 illustrates that every anion "connects" a ligand on the *x* axis of one $Cu(PyO)_6^{2+}$ complex with a ligand on the *y* axis from a neighboring complex. The fact that these pair spectra only occur in the NO_3^- system and not in the other two can be understood with this model since the NO_3^- ion with its π-system is well-known to provide a better exchange pathway than the tetrahedral ClO_4^- and BF_4^- ions with their sp^3 orbitals. In addition, the larger value of the coupling constant of this next-nearest-neighbor pair, relative to the nearest-neighbor interaction described by J', can be rationalized: as described above, the former constant describes the coupling between two orbitals that contain an unpaired electron ($d_{x^2-y^2}$), while the latter describes the coupling between $d_{x^2-y^2}$ and the doubly filled d_{z^2} orbital. As a consequence, the exchange coupling is much larger although the distance between the copper centers is much larger.

Registry No. $Cu(PyO)_6^{2+}$, 47839-68-9.

Contribution from the Departments of Chemistry,
University of Tennessee,
Knoxville, Tennessee 37996-1600,
and North Carolina State University,
Raleigh, North Carolina 27695-8204

Electrosynthesis and X-ray Structure of a Dinuclear Rhodium Complex Containing a Bridging Nitrate Ion

Louis J. Tortorelli,[1a] Craig A. Tucker,[1b] Clifton Woods,*[1a] and John Bordner[1c]

Received October 29, 1985

In recent years there has been considerable interest in dinuclear rhodium complexes containing bidentate bridging ligands where the donor atoms are those of group 15 elements.[2] One aspect of these complexes that has been a point of focus has been the wide range of metal-metal separations that can be achieved with ligands such as bis(diphenylphosphino)methane (dppm), bis(diphenylarsino)methane (dam), (diphenylarsino)(diphenylphosphino)methane (dapm), and 2-(diphenylphosphino)pyridine (Ph_2Ppy).

The dinuclear rhodium(I) complex $Rh_2(\mu\text{-}Ph_2Ppy)_2(\mu\text{-}CO)Cl_2$ (**1**) has been prepared and structurally characterized.[3] It has

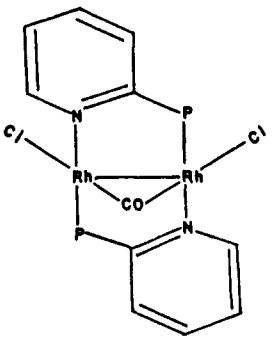

been noted that the geometric constraints of two bridging Ph_2Ppy ligands in a dinuclear complex limit the metal-metal separations to the metal-metal bond range,[4] and indeed **1** contains a Rh-Rh bond of 2.612 Å. If the bridging CO is viewed as a neutral ligand, the rhodium atoms in **1** are formally rhodium(I). When rhodium(I) dimers that lack a formal Rh-Rh bond and contain bridging dppm, dam, and dapm ligands undergo oxidative addition of molecules such as iodine, bromine, or CH_3SSCH_3,[5,6] the Rh-Rh separation decreases with the formation of a Rh-Rh bond.

Due to the small number of dinuclear rhodium(II) complexes that exists with bridging dppm, dam, dapm, and Ph_2Ppy ligands, we have been interested in investigating the possibility of making rhodium(II) complexes via electrochemical oxidation and assessing the role these electron-transfer processes play in the formation and stability of the Rh-Rh bond. One comparison of potential interest is that of the rhodium-rhodium bond distances in dinuclear rhodium(I) compounds, such as **1**, and those of their dinuclear rhodium(II) derivatives. Such comparisons might shed more light on how various geometric and steric constraints and electronic factors affect the metal-metal bond distances in these dinuclear rhodium complexes.

Experimental Section

Preparation of Compounds. Procedures outlined in the literature were used to prepare Ph_2Ppy[7] and $Rh_2(\mu\text{-}Ph_2Ppy)_2(\mu\text{-}CO)Cl_2$.[4]

$Rh_2(Ph_2Ppy)_2(\mu\text{-}NO_3)(CO)Cl_3\cdot CH_2Cl_2$ (2). Approximately 100-150 mg of $Rh_2(\mu\text{-}Ph_2Ppy)_2(\mu\text{-}CO)Cl_2$ was dissolved in 50 mL of CH_2Cl_2 containing 0.10 M tetra-*n*-butylammonium nitrate (TBAN) and a 5-fold molar excess of tetra-*n*-butylammonium chloride (TBAC). The solution was oxidized at 1.00 V (vs. SCE). After the oxidation was complete, the solution was washed with copious amounts of water to remove the TBAN and TBAC. The CH_2Cl_2 layer was reduced in volume on a rotary evaporator, and a greenish product was precipitated with ether and recrystallized from CH_2Cl_2/ether (yield 70%). If the oxidized solution is stripped to dryness and the residue is dissolved in acetone, the desired product can be obtained in comparable yield by the addition of water.

This compound can also be prepared by carrying out the same procedure as outlined above excluding the TBAC. Under these conditions, when ether is added to the CH_2Cl_2 that remains after washing with water to reach a cloud point, a brown product precipitates. Filtration followed by the addition of more ether to the filtrate afforded the desired product in 30% yield.

Electrochemistry. Cyclic voltammetry, coulometry, and controlled-potential electrolysis were performed with a BAS-100 electrochemical analyzer. The working electrode for cyclic voltammetry was a platinum-inlay electrode (Beckman), and the auxiliary electrode was a platinum grid. The working electrode for bulk electrolysis was a 25-cm^2 platinum grid, and the auxiliary electrode was a carbon rod. The reference electrode in all electrochemistry experiments was a saturated calomel electrode (SCE). All solutions were degassed with argon.

Physical Measurements. Infrared (IR) spectra were recorded as Nujol mulls on a Perkin-Elmer 180 infrared spectrophotometer. Proton-decoupled ^{31}P and ^{13}C NMR spectra were recorded on a JEOL FX90Q Fourier transform spectrometer. The ^{13}C NMR spectra were measured at 22.51 MHz with $(CH_3)_4Si$ as an external reference, and the ^{31}P NMR spectra were obtained at 36.19 MHz with 85% H_3PO_4 as the external reference. All spectra were obtained at ambient temperatures.

Single-Crystal X-ray Analysis.[8] The ruby-colored prismatic crystals of $Rh_2(\mu\text{-}Ph_2Ppy)_2(\mu\text{-}NO_3)(CO)Cl_3\cdot CH_2Cl_2$ were grown by the slow diffusion of ether into a CH_2Cl_2 solution of **2**. A representative crystal was surveyed, and a 1-Å data set (maximum $(\sin\theta)/\lambda = 0.5$ Å^{-1}) was collected. Crystal parameters are listed in Table I. Atomic scattering factors were taken from ref 9 except those for hydrogen, which were taken from Stewart, Davidson, and Simpson[10] and those for rhodium, which were taken from Cromer and Mann.[11] All crystallographic calculations were facilitated by the CRYM system.[12] All diffractometer

(1) (a) University of Tennessee. (b) North Carolina State University. (c) Formerly of North Carolina State University; currently at Pfizer Pharmaceutical.
(2) The groups of the periodic table are numbered according to recent recommendations from the IUPAC and ACS committees on nomenclature.
(3) Farr, J. P.; Olmstead, M. M.; Hunt, C. H.; Balch, A. L. *Inorg. Chem.* **1981**, *20*, 1182.
(4) Balch, A. L.; Guimerans, R. R.; Linehan, J.; Wood, F. E. *Inorg. Chem.* **1985**, *24*, 2021.
(5) Olmstead, M. M.; Balch, A. L. *J. Am. Chem. Soc.* **1976**, *98*, 2354.
(6) Balch, A. L.; Labadie, J. W.; Delker, G. *Inorg. Chem.* **1979**, *18*, 1224.
(7) Mann, F. G.; Watson, J. *J. Org. Chem.* **1948**, *13*, 502.
(8) Space group $P2_1/c$; $a = 11.863$ (8), $b = 17.076$ (5), $c = 19.430$ (8) Å; $Z = 4$; Syntex $P\bar{1}$ diffractometer; Mo Kα, $\lambda = 0.71069$ Å; 3577 reflections, $I > 1.0\sigma(I)$; 469 parameters; $R = 0.046$. Other crystal data and refinement details are available as supplementary data.
(9) *International Tables for X-ray Crystallography*; Kynoch: Birmingham, England, 1962; Vol. III, pp 204, 214.
(10) Stewart, R. F.; Davidson, E. R.; Simpson, W. T. *J. Chem. Phys.* **1965**, *42*, 3175.
(11) Cromer, D.; Mann, J. B. Report LA-3816; Los Alamos Scientific Laboratory: Los Alamos, NM, 1976.

0020-1669/86/1325-3534$01.50/0

Table I. Single Crystal X-ray Crystallographic Analysis[a]

A. Crystal Parameters	
formula (dimer + solvent)	$C_{36}H_{30}Cl_5N_3O_4P_2Rh_2$ (1013.8)
crystallizn medium	methylene chloride
cryst size, mm	0.30 × 0.30 × 0.50
cell dimens	
a, Å	11.863 (8)
b, Å	17.076 (5)
c, Å	19.430 (8)
β, deg	92.8 (2)
V, Å^3	3933 (2)
space group	$P2_1/c$
molecules/unit cell	4
density obsd, g/cm^3	1.65
density calcd, g/cm^3	1.712
linear abs coeff, cm^{-1}	10.93
transmission factors (max, min)	0.720, 0.488
B. Refinement Parameters	
no. of reflcns	4322
no. of nonzero reflcns ($I > 1.0\sigma$)	3577
R index = $\sum\|\|F_o\| - \|F_c\|\|/\sum\|F_o\|$	0.46
R_w	0.00736
GOF = $[\sum w(F_o^2 - F_c^2)^2/(m - s)]^{1/2}$	1.88
scale factor	0.937 (2)
no. of parameters	469

[a] Due to the small absorption coefficient, absorption corrections were not made. The maximum and minimum transmission factors were calculated by using the shortest and longest path lengths through the crystal, respectively.

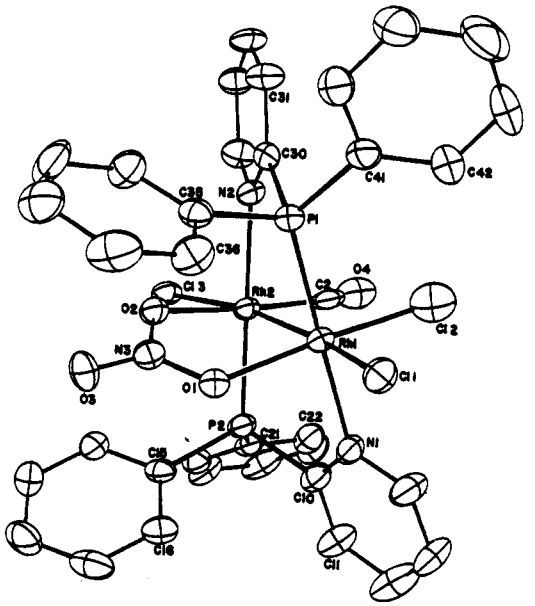

Figure 1. ORTEP plot of $Rh_2(\mu\text{-}Ph_2Ppy)_2(\mu\text{-}NO_3)(CO)Cl_3$ showing the numbering scheme. In the cases of phenyl groups and pyridine rings, the numbers of the carbon atoms increase sequentially around the rings.

data were collected at room temperature.

A trial structure was obtained by conventional Patterson and Fourier techniques. This trial structure refined routinely. Hydrogen positions were calculated by using idealized parameters. The hydrogen parameters were added to the structure factor calculations but were not refined. The final cycles of full-matrix least-squares refinement contained the scale factor, coordinates, and anisotropic temperature factors in a single matrix. The shifts calculated in the final cycle were zero. A secondary extinction correction was attempted but refined to a value of zero. The refined structure was plotted by using the ORTEP computer program of Johnson.[13] Atomic positional coordinates are listed in Table IV; anisotropic temperature factors, complete bond distances and angles, and observed and calculated structure factors are available as supplementary material.

A final difference Fourier analysis revealed residual electron density between the carbonyl, one of the chlorines, Cl(2), and the rhodium atoms (Figure 1). In addition, the refined carbon–oxygen bond length in the carbonyl was remarkably short (0.835 Å). The temperature factors for these three atoms (C(2), O(4), and Cl(2)) were much larger than other temperature factors in the molecule. This indicated the possibility that these two groups could be disordered. The trial structure was modified to include both groups on both rhodium atoms. A population of 0.5 was assigned to the groups. Least-squares refinement showed that this model fit the data as well as the one reported. However, bond distances were not greatly improved and in fact were more unreasonable. The simpler of the two models is reported, but the accuracy for the bond lengths and angles when the carbonyl and chlorine atom Cl(2) are involved is questionable. This uncertainty is caused by a disorder in the crystal that cannot be reasonably fit with a simple model.

Table IV. Coordinates (×10^4) and Their Standard Deviations

	x/a	y/b	z/c
Rh(1)	7381 (1)	9814 (0)	1949 (0)
Rh(2)	7337 (1)	10142 (0)	3248 (0)
Cl(1)	7382 (2)	9253 (1)	766 (1)
Cl(2)	8155 (2)	10999 (2)	1655 (1)
Cl(3)	7084 (2)	10225 (1)	4512 (1)
Cl(4)	8824 (6)	2126 (4)	5191 (3)
Cl(5)	11166 (6)	2186 (5)	5238 (3)
P(1)	9066 (2)	9221 (1)	2170 (1)
P(2)	5446 (2)	10311 (1)	3088 (1)
N(1)	5761 (5)	10378 (4)	1715 (3)
N(2)	9138 (5)	9977 (4)	3410 (3)
N(3)	6695 (5)	8517 (4)	2853 (4)
O(1)	6534 (4)	8809 (3)	2242 (3)
O(2)	7185 (4)	8925 (3)	3340 (3)
O(3)	6383 (5)	7851 (3)	2970 (3)
O(4)	7760 (6)	11752 (4)	3157 (4)
C(1)	9976 (20)	2609 (13)	4958 (10)
C(2)	7614 (6)	11274 (6)	3157 (4)
C(10)	5042 (7)	10581 (5)	2200 (4)
C(11)	4026 (8)	10969 (6)	2021 (5)
C(12)	3752 (8)	11140 (6)	1340 (5)
C(13)	4489 (8)	10938 (6)	858 (5)
C(14)	5486 (8)	10548 (6)	1057 (5)
C(15)	4645 (6)	9415 (5)	3238 (4)
C(16)	3993 (7)	9053 (5)	2713 (4)
C(17)	3443 (7)	8355 (5)	2827 (5)
C(18)	3502 (8)	8009 (5)	3478 (6)
C(19)	4147 (8)	8373 (6)	3998 (5)
C(20)	4730 (7)	9057 (5)	3895 (5)
C(21)	4829 (6)	11090 (5)	3597 (4)
C(22)	4229 (7)	10942 (5)	4167 (5)
C(23)	3814 (8)	11543 (6)	4555 (5)
C(24)	3995 (9)	12309 (6)	4365 (5)
C(25)	4605 (9)	12468 (5)	3799 (5)
C(26)	5015 (7)	11862 (5)	3408 (5)
C(30)	9788 (6)	9602 (5)	2965 (4)
C(31)	10931 (7)	9480 (5)	3118 (5)
C(32)	11424 (7)	9761 (5)	3725 (5)
C(33)	10775 (7)	10174 (5)	4162 (4)
C(34)	9649 (7)	10279 (5)	3982 (4)
C(35)	8953 (6)	8168 (5)	2326 (4)
C(36)	8507 (7)	7708 (5)	1792 (5)
C(37)	8439 (8)	6896 (6)	1880 (5)
C(38)	8820 (8)	6547 (5)	2483 (6)
C(39)	9250 (8)	7008 (6)	3015 (5)
C(40)	9309 (7)	7815 (5)	2944 (5)
C(41)	10174 (6)	9268 (5)	1547 (4)
C(42)	10265 (8)	9907 (6)	1100 (5)
C(43)	11154 (9)	9936 (6)	670 (5)
C(44)	11941 (9)	9362 (7)	671 (5)
C(45)	11882 (8)	8733 (7)	1102 (5)
C(46)	10988 (8)	8675 (6)	1534 (5)

Results and Discussion

Synthesis. The cyclic voltammogram of **1** in CH_2Cl_2 containing 0.10 M tetra-*n*-butylammonium hexafluorophosphate (TBAH) reveals irreversible oxidation peaks at +0.82 and +1.11 V (Figure 2A). Upon sweeping through these oxidation peaks, one observes

(12) Duchamp, D. J. Paper B-14, American Crystallographic Association Meeting, Boseman, MT, 1964; p 29.
(13) Johnson, C. K. ORTEP Report ORNL-3794; Oak Ridge National Laboratory: Oak Ridge, TN, 1965.

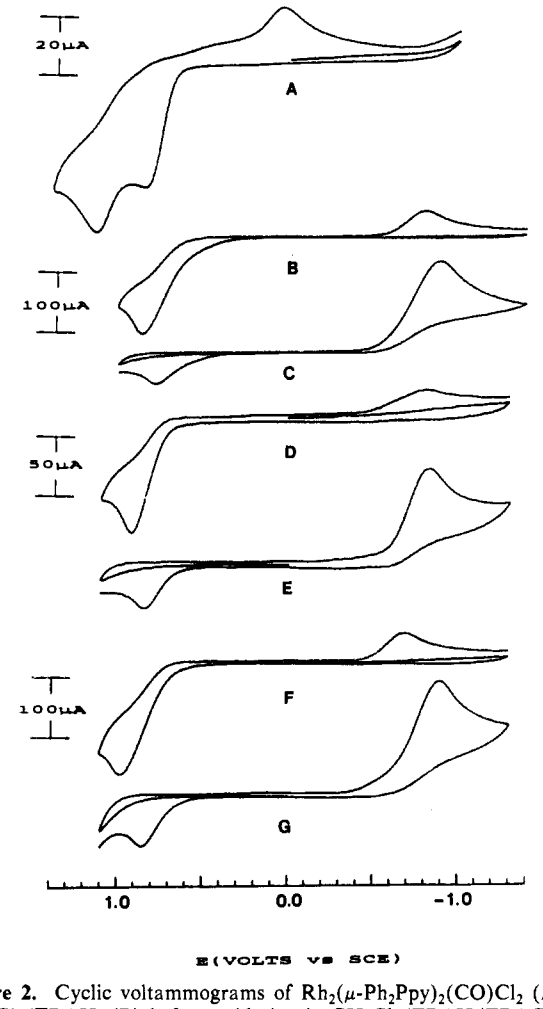

Figure 2. Cyclic voltammograms of $Rh_2(\mu\text{-}Ph_2Ppy)_2(CO)Cl_2$ (A) in CH_2Cl_2/TBAH, (B) before oxidation in CH_2Cl_2/TBAH/TBAC, (C) after oxidation in CH_2Cl_2/TBAH/TBAC, (D) before oxidation in CH_2Cl_2/TBAN, (E) after oxidation in CH_2Cl_2/TBAN, (F) before oxidation in CH_2Cl_2/TBAN/TBAC, and (G) after oxidation in CH_2Cl_2/TBAN/TBAC.

a reduction peak at 0.0 V. Though controlled-potential electrolysis at +1.30 V corresponds to a total of two electrons transferred per dimer, no product has yet been isolated or characterized.

In view of some results we previously reported showing that coordinating species add to rhodium dimers similar to **1** during electrochemical oxidation,[14,15] we performed the electrochemical oxidation of **1** in CH_2Cl_2/TBAH containing a 5-fold excess of TBAC with the hope of being able to isolate a Rh(II)–Rh(II) dimer. With the free Cl^- present, the cyclic voltammogram exhibits a single two-electron irreversible peak at +0.86 V and a corresponding reduction peak at −0.78 V (Figure 2B). After oxidation at +0.95 V, an irreversible reduction peak occurs at −0.88 V (Figure 2C). Again, attempts to characterize the oxidation product have thus far been unsuccessful.

In attempts to isolate an oxidation product of **1**, TBAH was replaced with TBAN as the supporting electrolyte. The cyclic voltammogram of **1** in CH_2Cl_2/TBAN exhibits an irreversible oxidation peak at +0.90 V and a corresponding reduction peak at −0.82 V (Figure 2D). Coulometry indicates that the oxidation is a two-electron process, apparently leading to a Rh(II)–Rh(II) dimer. The oxidation product gives rise to a reduction wave at −0.81 V. When the solution contains free Cl^-, the oxidation peak occurs at +0.97 V. The cyclic voltammogram of **1** in the chloride-containing medium reveals that the initial oxidation product exhibits a reduction wave at −0.70 V, suggesting that on the cyclic voltammetric time scale the oxidation product formed in the presence of Cl^- is less stable to reduction than the one formed in the absence of Cl^-. However, when bulk electrolysis is performed at +1.0 V, the product produced on the electrolysis time scale exhibits a reduction wave at −0.84 V (Figure 2E). This potential shift suggests that the initial oxidation product undergoes a slow chemical transformation leading to the isolated product.

Identical products are isolated from the two electrolysis media, CH_2Cl_2/TBAN (30% yield) and CH_2Cl_2/TBAN/TBAC (70% yield); however, the CH_2Cl_2/TBAN medium also affords a brown product, which so far has eluded characterization. The IR spectrum of the desired product exhibits a carbonyl stretching frequency at 2054 cm^{-1}, indicating the presence of a terminal carbonyl ligand. The presence of a terminal CO means that the two rhodium environments are different, and therefore, the environments of the two phosphorus atoms on the two bridging Ph_2Ppy ligands are different.

The $^{31}P\{^1H\}$ NMR spectrum of the Rh(II) dimer consists of two doublets of doublets with chemical shifts at 33.0 and 28.7 ppm (relative to 85% H_3PO_4). The larger coupling, ^1J(P–Rh), for the downfield multiplet is 114.7 Hz and that for the upfield multiplet is 119.6 Hz. The smaller splitting in each case is 17.1 Hz. In order to assign the phosphorus resonances, the complex was prepared with ^{13}C-enriched CO. Only the downfield doublet of doublets exhibits the effects of ^{13}C coupling, indicating that the CO and the phosphorus nucleus giving rise to the downfield multiplet are coordinated to the same rhodium atom. With ^{13}CO, the downfield doublet of doublets appears as a pseudo doublet of triplets since the ^2J(P–C) value of 14.7 Hz is close enough to the smaller coupling of the downfield multiplet that the two center lines of the new doublets overlap and give rise to a three-line pattern.

X-ray Crystal Structure of $Rh_2(\mu\text{-}Ph_2Ppy)_2(\mu\text{-}NO_3)(CO)Cl_3\cdot CH_2Cl_2$. An ORTEP plot of the dinuclear species with the atomic numbering scheme is shown in Figure 1. Complex **2** contains two Rh(II) d^7 metal centers surrounded by ligating atoms that form two interpenetrating irregular octahedra held together by the two bridging transoid Ph_2Ppy ligands in a head-to-tail arrangement, a bridging nitrate ion, and a metal–metal bond. Each rhodium atom is located in the center of an irregular octahedron such that each Rh atom occupies a vertex of the octahedron surrounding the other Rh atom. A chlorine atom is coordinated to each rhodium atom such that the two chlorine atoms are tilted away from the Rh–Rh vector toward the bridging nitrate by 10°. One rhodium atom is located at the intersection of two essentially perpendicular (179.5°) vectors, a PRhN vector (P and N from two transoid Ph_2Ppy ligands) and an ORhCO vector (O from μ-NO_3). The second rhodium is also located at the intersection of two essentially perpendicular (178.9°) vectors, a PRhN vector and an ORhCl vector (O from μ-NO_3). When **2** is viewed down the Rh–Rh axis, it is seen that the ligating atoms on the two metals are in a staggered orientation with a torsional angle of 13.79°. The skewing of the PRhN units is not surprising since the A-frame precursor, $Rh_2(\mu\text{-}Ph_2Ppy)_2(\mu\text{-}CO)Cl_2$, exhibits significant skewing of the PRhN units.[3] This skewing has been related to the bite of the Ph_2Ppy ligand. An idealized Rh–Rh separation of 2.35 Å has been determined for a planar $(Ph_2Ppy)_2M_2$ unit in which each Ph_2Ppy ligand bridges the two metal atoms. The skewing in **2** is undoubtedly induced by the metal–metal bond distance of 2.589 Å. This distance is shorter than the metal–metal distance of 2.612 Å observed for the A-frame rhodium(I) precursor. This decrease in Rh–Rh bond distance apparently results from the increase in metal–metal bonding interactions that occur upon removal of electrons from essentially a $d_{z^2}(\sigma^*)$ orbital during the oxidation of the metal centers.

The only anomalous feature of the structure is the C–O distance of the carbonyl group. The anomalous value of 0.835 Å results from a disorder involving the CO on one rhodium atom and the staggered Cl on the second rhodium atom. A similar type of disorder involving trans carbonyl and chloro ligands on the same rhodium atom has previously been observed.[16] The disorder in

(14) Womack, D. R.; Enlow, P. D.; Woods, C. *Inorg. Chem.* **1983**, *22*, 2653.
(15) Enlow, P. D.; Woods, C. *Inorg. Chem.* **1985**, *24*, 1273.
(16) La Placa, S. J.; Ibers, J. A. *J. Am. Chem. Soc.* **1965**, *87*, 2581.

2 apparently results when some molecules crystallize with the carbonyl and chloro ligands having exchanged coordination sites. This can be achieved by simply rotating the molecule 180° about a vector bisecting the Rh–Rh bond and the O(1)–N(3)–O(2) angle. A model consisting of a half Cl and a half CO at each site fits the data as well as the one with the CO totally contained in one site and the Cl in the other site. Because of this disorder the C–O and the Rh(1)–Cl(2) distances cannot be determined accurately.

Concluding Remarks. We have further demonstrated that electrochemical oxidation of dinuclear rhodium(I) complexes in the presence of coordinating ligands can lead to novel rhodium(II) dimers. An increase in the oxidation state from Rh(I) to Rh(II) is generally accompanied by an increase in coordination number. In the present case it is somewhat interesting that though Cl^- is generally considered to be a better coordinating ligand for transition metals than NO_3^-, the dinuclear Rh(I) species adds a Cl^- and a NO_3^- instead of two Cl^- ions. It is also interesting to note that, even in the absence of an external source of Cl^-, oxidation of **1** in the CH_2Cl_2/TBAN medium still affords compound **2**. Either the starting material or some other rhodium-containing species serves as the source of the additional chloride found in **2**. This is apparently the reason for the lower yield of **2** under these conditions. The solvent, CH_2Cl_2, is not the source of Cl^- since the same results are obtained with the medium $(CH_3)_2CO$/TBAN.

It is possible that the addition of the bridging NO_3^-, instead of a bridging Cl^- for instance, may result from the ability of the bridging nitrate to accommodate the twist angle (see Figure 1) imposed by the Ph_2Ppy ligands while still allowing each rhodium to have an electron count of 18. Studies that probe the relationship between geometric constraints and the relative coordination abilities of nitrate and other donors are being conducted.

Acknowledgment. We wish to thank the National Science Foundation for support of this work and Johnson Matthey, Inc., for their generous loan of rhodium trichloride. We also extend our thanks to Dr. George M. Brown of Oak Ridge National Laboratory for his helpful comments.

Registry No. **1**, 75361-61-4; **2**, 103438-59-1; TBAN, 1941-27-1; TBAC, 1112-67-0; TBAH, 3109-63-5; Rh, 7440-16-6.

Supplementary Material Available: Tables II, III, and V, giving complete bond distances and angles, hydrogen atom coordinates, and anisotropic temperature factors (5 pages); Table VI, giving observed and calculated structure factors (18 pages). Ordering information is given on any current masthead page.

Contribution from the Departments of Chemistry, Texas A&M University, College Station, Texas 77843, and University of Delaware, Newark, Delaware 19716

Chemical and Structural Characterization of $W(CO)_5OPPh_2NPPh_3$. A Novel Complex Containing a Phosphine Oxide Ligand Derived from the Bis(triphenylphosphine)nitrogen(1+) Cation

Donald J. Darensbourg,*[1a] Magdalena Pala,[1a] Debra Simmons,[1a] and Arnold L. Rheingold*[1b]

Received March 7, 1986

There is wide-spread advance of the intermediacy of low-valent metal–alkoxides[2-7] and –alkoxycarbonyl[8-15] species in homogeneous-catalyzed reactions. An illustrative and pertinent example to our research efforts is the methanol carbonylation to methyl formate process employing group 6 or 8 metal carbonyl catalysts.[16,17] Nevertheless, there are few reports of isolated and well-characterized alkoxide derivatives of zerovalent group 6 metals, and all of these are polynuclear.[18-20] One of these species is an anionic chromium tetramer recently reported by McNeese and co-workers.[20] The alkoxide derivative was obtained from the reaction of chromium hexacarbonyl and excess hydroxide ion in refluxing methanol. This tetraanion has a cubane-like structure comprised of four $[Cr(CO)_3(OCH_3)]^-$ monomers, where the Cr_4O_4 core is a distorted cube with chromium and methoxide oxygen atoms occupying alternate corners.[21]

Preliminary results from our laboratories demonstrate that these species react reversibly with carbon monoxide in THF to provide the mononuclear derivatives, with results being unequivocal for the process described in eq 1.[22] The species $W(CO)_5$[OPh][PPN] has previously been reported to be formed from the reaction of $W(CO)_5$THF with [PPN][OPh].[23]

$$[W_4(CO)_{12}(\mu_3\text{-OPh})_4]^{4-} + CO \rightarrow 4W(CO)_5OPh^- \quad (1)$$

Our interest in fully characterizing low-valent group 6 methoxy- and carbonylmethoxy species as possible intermediates in methanol carbonylation processes prompted us to attempt the preparations of an anhydrous, aprotic solvent soluble salt of the methoxide ion. For this purpose the PPN^+ (bis(triphenylphosphine)nitrogen(1+)) cation is widely used in organometallic chemistry. Furthermore, it customarily affords stabilization, both in solution[24] and in the solid state,[25] to reactive transition-metal carbonyl anions. In

(1) (a) Texas A&M University. (b) University of Delaware.
(2) Bryndza, H. E.; Kretchman, S. A.; Tulip, T. H. *J. Chem. Soc., Chem. Commun.* **1985**, 977.
(3) Bryndza, H. E. *Organometallics* **1985**, *4*, 1686.
(4) Reese, W. M.; Atwood, J. D. *Organometallics* **1985**, *4*, 402.
(5) Newman, L. J.; Bergman, R. G. *J. Am. Chem. Soc.* **1985**, *107*, 5314.
(6) Gaus, P. L.; Kao, S. C.; Youngdahl, K. A.; Darensbourg, M. Y. *J. Am. Chem. Soc.* **1985**, *107*, 2428.
(7) Kao, S. C.; Gaus, P. L.; Youngdahl, K. A.; Darensbourg, M. Y. *Organometallics* **1984**, *3*, 1601.
(8) For reviews, see: (a) Falbe, J. *New Syntheses with Carbon Monoxide*; Springer: Berlin, 1980; p 226. (b) Roper, M.; Loevenich, H., In *Catalysis in C_1 Chemistry*; Keim, W., Ed.; D. *Reidel*: Dordrecht, The Netherlands, 1983; p 105.
(9) Milstein, D.; Huckaby, J. L. *J. Am. Chem. Soc.* **1982**, *104*, 6150.
(10) Wood, C. D.; Garrou, P. E. *Organometallics* **1984**, *3*, 170.
(11) Tasi, M.; Palyi, G. *Organometallics* **1985**, *4*, 1523.
(12) Gross, D. C.; Ford, P. C. *Inorg. Chem.* **1982**, *21*, 1702.
(13) Anstock, M.; Taube, D.; Gross, D. C.; Ford, P. C. *J. Am. Chem. Soc.* **1984**, *106*, 3696.
(14) Gross, D. C.; Ford, P. C. *J. Am. Chem. Soc.* **1985**, *107*, 585.
(15) Trautman, R. J.; Gross, D. C.; Ford, P. C. *J. Am. Chem. Soc.* **1985**, *107*, 2355.
(16) Darensbourg, D. J.; Gray, R. L.; Pala, M. *Organometallics* **1984**, *3*, 1928.
(17) Darensbourg, D. J.; Gray, R. L.; Ovalles, C.; Pala, M. *J. Mol. Catal.* **1985**, *29*, 285.
(18) Kirtley, S. W.; Chanton, J. P.; Love, R. A.; Tipton, D. L.; Sorrell, T. N.; Bau, R. *J. Am. Chem. Soc.* **1980**, *102*, 3451.
(19) Ellis, J. E.; Rochfort, G. L. *Organometallics* **1982**, *1*, 682.
(20) McNeese, T. J.; Cohen, M. B.; Foxman, B. M. *Organometallics* **1984**, *3*, 552.
(21) McNeese, T. J.; Mueller, T. E.; Wierda, D. A.; Darensbourg, D. J.; Delord, T. J. *Inorg. Chem.* **1985**, *24*, 3465.
(22) Darensbourg, D. J.; Summers, K. M., results submitted for publication.
(23) Slater, S. G.; Lusk, R.; Schumann, B. F.; Darensbourg, M. Y. *Organometallics* **1982**, *1*, 1662.
(24) Darensbourg, M. Y.; Barros, H.; Borman, C. *J. Am. Chem. Soc.* **1977**, *99*, 1647.
(25) (a) Walker, H. W.; Ford, P. C. *J. Organomet. Chem.* **1981**, *214*, C43. (b) Jackson, P. F.; Johnson, B. F. G.; Lewis, J.; McPartlin, M.; Nelson, W. J. H. *J. Chem. Soc., Dalton Trans.* **1978**, 920. (c) Eady, C. R.; Johnson, B. F. G.; Lewis, J.; Malatesta, M. C.; Machin, P.; McPartlin, M. *J. Chem. Soc., Chem. Commun.* **1976**, 945. (d) Walker, H. W.; Pearson, R. G.; Ford, P. C. *J. Am. Chem. Soc.* **1983**, *105*, 1179. (e) Smith, M. B.; Bau, R. *J. Am. Chem. Soc.* **1973**, *95*, 2388. (f) Wilson, R. D.; Bau, R. *J. Am. Chem. Soc.* **1974**, *96*, 7601. (g) Handy, L. B.; Ruff, J. K.; Dahl, L. F. *J. Am. Chem. Soc.* **1972**, *92*, 7312. (h) Handy, L. B.; Treichel, P. M.; Dahl, L. F.; Hayter, R. G. *J. Am. Chem. Soc.* **1966**, *88*, 366. (i) Wilson, R. D.; Graham, S. A. Bau, R. *J. Organomet. Chem.* **1975**, *91*, C49.

0020-1669/86/1325-3537$01.50/0